Spatially Extended Avalanches in a Hysteretic Capillary Condensation System: Superfluid ^{4}He in Nuclepore

M. P. Lilly, A. H. Wootters, and R. B. Hallock

Laboratory for Low Temperature Physics, Department of Physics and Astronomy, University of Massachusetts, Amherst, Massachusetts 01003

(Received 31 May 1996)

Capacitive studies of hysteretic capillary condensation of superfluid ^{4}He in Nuclepore have shown that the initial draining of the pores occurs over a small range of the chemical potential with avalanches present as groups of pores drain. In the work reported here, the avalanches in this system are shown to be nonlocal events which involve pores distributed at low density across the entire sample. The nonlocal avalanche behavior is shown to be enabled by the presence of a superfluid film connection among the pores. [S0031-9007(96)01606-7]

PACS numbers: 67.70.+n, 47.55.Mh, 67.40.Hf, 68.45.Da

Avalanche events have been observed in Martensitic transformations [1], mercury injection [2], and magnetic phenomena, including Barkhausen noise [3], and vortex motion [4] in superconducting cylinders and thin superconducting films, etc. Theoretical studies of interacting hysteretic magnetic systems find that interactions among magnetic domains give rise to avalanches, and that the avalanche characteristics are predicted to depend on the strength of the interactions among the domains relative to the strength of the disorder [5]. Hysteresis models for capillary condensation include *local* pore-to-pore interaction [6,7] via interconnections. Capillary condensation studies of ordinary adsorptive fluids in porous systems [8,9] have not shown avalanche behavior.

Studies of superfluid ^{4}He in Nuclepore [10] show that the adsorption isotherms are hysteretic [11–14] due to the metastability of the configuration of the helium in the pores [15] and that avalanches occur during pore draining [11,16]. Here we report measurements of the spatial extent of these avalanches, and find that the avalanche events in this system are *not local events*, but involve a low density of pores widely distributed over the macroscopic sample [17], a result contrary to expectations based on local interaction models. We use ^{4}He as the working fluid due to its purity, the ability to utilize its behavior for an *in situ* monitor of the chemical potential, and the presence of a superfluid density, which allows us to change the dynamical behavior of the working fluid. Our experiments show that the avalanches and their nonlocal behavior are enabled by the superfluid characteristics of the ^{4}He.

Nuclepore is a 10 μm thick polycarbonate membrane which has a random spatial distribution of nearly cylindrical pores of nominal diameter 200 nm. A pore density, $\psi \approx 3 \times 10^8$ pores/cm^2, and a random tilt angle, θ, of the axis of each pore from the normal to the surface, $0° \leq \theta \lesssim 34°$, lead to a large number of intersections among the pores in the sample. Computer simulations with these parameters indicate an average of five intersections per pore [11] and a percolated network of pores; the cluster size is macroscopic. This material, with controlled pore sizes, access to the macroscopic sample surface for *every* pore, and relatively uniform pore shapes, gives us the opportunity to study events associated with capillary condensation in a relatively simple (but not trivial) porous material.

The amount of ^{4}He in the Nuclepore is measured with a capacitance technique. Ag capacitor plates of thickness 50 nm are thermally evaporated on either side of the Nuclepore membrane. Scanning electron microscope photographs show that the Ag does not close or significantly modify the pore openings. Because ^{4}He is a dielectric, the capacitance, C, shifts as atoms enter the pores. Assuming cylindrical pores of radius R, the change in capacitance associated with a fraction, f, of the pores capillary condensed is $\Delta C \approx \epsilon_0 A[f + 2(1 - f)d_p/R](1 - f_N) \times (\kappa_{\mathrm{He}} - 1)/t$ where A is the area of each capacitor plate, d_p is the helium film thickness in an unfilled pore, t is the thickness of the Nuclepore, f_N is the fraction of the volume between the capacitor plates filled with polycarbonate (i.e., excluding the pores), and $\kappa_{\mathrm{He}} = 1.055$ is the dielectric constant of liquid helium. The capacitance is measured with a self-balancing bridge with resolution $\delta C/C \sim 5 \times 10^{-8}$.

A Nuclepore sample (200 nm diam pores) and a borosilicate glass third sound substrate are sealed in a 78 cm^3 Cu sample chamber along with a superfluid film reservoir consisting of ~200 sheets of Nuclepore with 400 nm diam pores which provides a surface area $A_r \sim 4.9$ m^2. The sample chamber is attached by a weak thermal link to a continuously pumped ^{4}He refrigerator maintained at a temperature T_0. For the data discussed here, the sample chamber temperature is regulated at $T_r \approx T_0 + 0.045$ K, with $T_r < T_\lambda = 2.17$ K, by using a heater and an integrating temperature controller. This allows temperature regulation for up to 6 days with long-term stability $\delta T \sim 250$ μK, which is adequate for our experiments. To change the chemical potential at fixed T_r, we slowly and continuously add or remove ^{4}He gas through a room temperature metering valve with flow rates selected so as to avoid relaxation and thermal effects.

 0031-9007/96/77(20)/4222(4)$10.00

The chemical potential is determined *in situ* by measuring the velocity of third sound on the borosilicate glass slide in the sample chamber, a technique used previously [13,14]. Third sound is a temperature and thickness wave on a superfluid ^{4}He film with a velocity that is a sensitive function of the chemical potential near the saturated vapor pressure. The third sound velocity is parametrized by [18]

$$C_3^2 = \left\langle \frac{\rho_s}{\rho} \right\rangle \left[1 + \frac{TS}{L} \right]^2 \frac{\alpha\beta(4d + 3\beta)}{d^3(d + \beta)^2}, \qquad (1)$$

where α is the van der Waals constant, β a retardation parameter, d the film thickness, S the entropy, L the latent heat, and $\langle \rho_s/\rho \rangle$ the effective superfluid fraction. To carry out these velocity measurements, we repetitively apply a zero-offset square voltage pulse to a 30 nm thick Ag thermal driver and digitize and signal average the resulting voltage signal from a superconducting transition-edge Al bolometer. The measured time of flight of the third sound pulse and the known distance between the driver and detector give the velocity. We numerically invert Eq. (1) to find d, and thus monitor the chemical potential by the use of $\mu_f - \mu_0 = -\alpha\beta/[d^3(d + \beta)]$, where μ_0 is the chemical potential of bulk liquid.

The measured capacitance as a function of chemical potential yields a global hysteresis loop for a typical isotherm as shown in Fig. 1(a). The lower (upper) curve are data for adding (removing) ^{4}He to (from) the sample chamber. For both adding and removing ^{4}He, rates were low enough to avoid relaxation effects. The total change in capacitance from empty (691.157 pF) to full (695.190 pF) is 4.033 pF. On ^{4}He removal, pores drain rapidly over a very narrow range of the chemical potential for $\mu - \mu_0 \lesssim -0.013$ K. One possible explanation of this drop is that the pores have a narrow distribution of pore diameters, and therefore will drain at nearly the same chemical potential. This behavior is expected in a system where the pores act independently (Preisach model). Observations with hysteresis subloops [11,19] indicate that this simple model is inadequate, and that interactions are present among the pores. One interaction mechanism, often invoked in porous studies, is pore blocking [9], a situation in which internal pores have no direct access to the vapor phase due to the presence of intervening filled pores. In the case of Nuclepore, pore blocking was not expected to occur since *each* pore has access to the surface and the chemical potential of the vapor. The pores, however, are slightly barrel shaped [12–14,20]. Because of the multiple intersections among the pores in the interior of the material, it is possible to have large intersection openings in the interior blocked by smaller openings at the surface, which will limit draining until such internal pore openings have access to the surface [19].

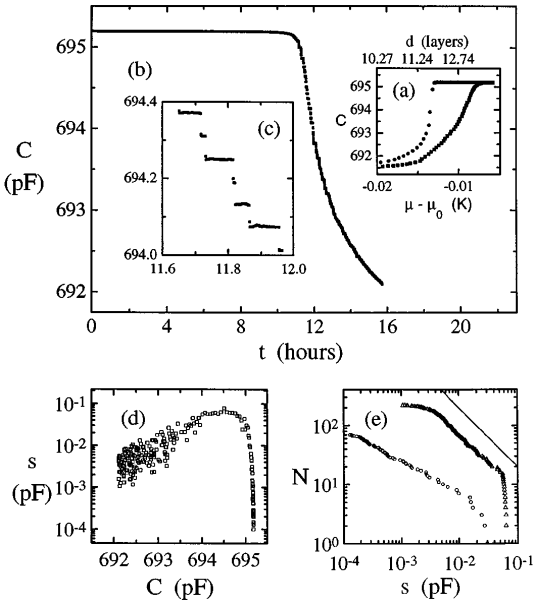

FIG. 1. (a) Hysteresis for filling (squares) and draining (circles) ^{4}He in Nuclepore. Avalanches are only observed during draining. (b) and (c) Steps in the capacitance are observed during slow removal of ^{4}He ($\partial\mu/\partial t = -1.6 \times 10^{-7}$ K/sec) while monitoring the capacitance at a rate of $\sim$1 measurement/sec for $T_r = 1.476$ K. (d) The avalanche size as a function of the amount of ^{4}He in the pores. (e) N is the total number of avalanches of size larger than s. Data represented by circles (triangles, top) are data for the initial (later) part of the draining. N vs s for the entire data set resembles the triangles. The solid line is $N \sim s^{-1}$.

To document the details of pore draining, we monitor the capacitance as a function of time while very slowly removing ^{4}He. An example of draining is shown in Fig. 1(b), where we measure $\sim 1.9 \times 10^4$ capacitance values in $\sim$16 hours. The capacitance drops in a series of steps [11,16] indicating that the pores are draining in groups (i.e., avalanches) rather than one pore at a time. In this example, 218 avalanches which exceed our sensitivity limit are recorded as the pores drain. An expanded view of a small number of these avalanches is shown in Fig. 1(c). Although ^{4}He is removed from the pores in a short time during an avalanche, there are helium atoms in the vapor and the film reservoir which serve to limit the size of chemical potential changes in the cell caused by the avalanches. In Fig. 1(d), the size of the capacitance steps (avalanches) is plotted as a function of the capacitance value where each step begins. The beginning capacitance of a step is directly related to the fraction of pores filled with ^{4}He. We calculate the number of pores in an avalanche, N_a, from the fractional change in capacitance, $N_a = \psi A \Delta C/(C_{\text{full}} - C_{\text{empty}})$ where ΔC is the size of the capacitance step, and $C_{\text{full}} - C_{\text{empty}}$ is the total change in the capacitance associated with complete filling of the pores. For Fig. 1, $N_a/\Delta C = 2.6 \times 10^8$ pores/pF. This estimate for N_a neglects the small effect on the capacitance due to the presence of helium film on the cylindrical surface of the uncondensed pores.

The size distribution function, $D(s)$, where $D(s)ds$ is the probability of an avalanche occurring in the size range s to $s + ds$, can be used to characterize a set of avalanches. In Fig. 1(e), N is the total number of avalanches larger than size s. An advantage to using N is that the plot does not

depend on the specifics of an arbitrary binning procedure to get $D(s)$; no binning is used here. N is related to $D(s)$ by $N = N_t \int_s^\infty D(s)\, ds$, where N_t is the total number of avalanches. For cases where the withdrawal of ^{4}He from the cell proceeds very slowly, and the temperature is stable, we observe two regions of approximate power law behavior. In other cases, N vs s shows less distinct behavior. In the example of Fig. 1(d), for $C > 694.90$ pF, $N \sim s^{-0.54}$, and for $C < 694.90$ pF, $N \sim s^{-0.95}$. In each case, for $N \sim s^{-m}$ the size distribution is $D(s) \sim s^{-(m+1)}$.

Avalanche behavior on the draining part of the hysteresis loop is dramatically reduced when the system is brought to $T_r = 2.06$ K, and it can be eliminated by the addition of substantial ^{3}He to the ^{4}He working fluid. Given the present design of the cryostat, it is not possible to achieve adequate temperature stability for measurements above T_λ. In the case of mixtures, the withdrawal of helium from the cell by pumping necessarily means that the ^{3}He concentration in the cell is not maintained constant during a series of avalanches. In spite of these difficulties, it is clear that the avalanche structure is tunable by adjustment of the temperature or the ^{3}He concentration, and that the presence of superfluidity is relevant to the existence of the prompt multiple-pore avalanches in this system. Such tunability has been elusive in previous studies of avalanches in other systems.

Measurement of the sizes of the avalanches provides information about the total number of pores that drain between the capacitor plates in avalanche events, but does not indicate the spatial extent of the pores involved in an avalanche. To study the spatial extent of the avalanches, we created a second sample [17] which utilized two rectangular capacitors 4.8 mm $\times$ 20.2 mm separated by 3.2 mm on a single Nuclepore membrane (Fig. 2, inset). For convenience, the capacitance bridge sequentially sampled each capacitor using a fast switch. We have confirmed that the switch has no effect on the measurements by conducting simultaneous measurements with two independent bridges with different operating characteristics without switching. The results for a typical set of avalanches as measured by the two separate capacitors are shown in Fig. 2. This portion of the capacitance vs time is representative of the entire set of data and shows that avalanche events recorded by one capacitor are highly correlated in both size and time with avalanche events recorded by the other capacitor.

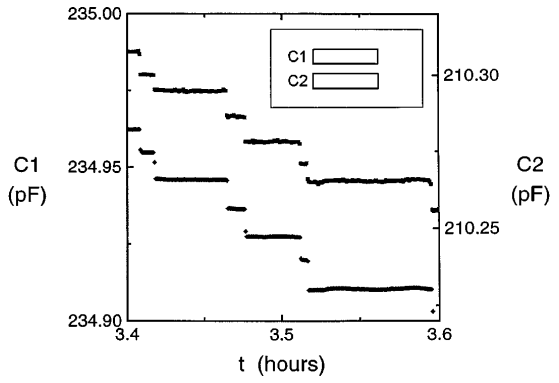

FIG. 2. Avalanche behavior for a pair of equal-sized capacitors, C1 (diamonds, bottom) and C2 (squares, top), located on a single piece of Nuclepore (inset) for $T_r = 1.451$ K. Avalanche events are highly correlated in size and in time.

One conclusion from the observation of highly correlated avalanches is that draining events do *not* involve localized regions of high pore density. That is, the avalanches do not involve single clusters of high density which are isolated from the rest of the sample. In Fig. 2, the largest avalanches are about $\sim$0.01 pF which corresponds to $\sim 2.6 \times 10^6$ pores. If all of these pores were adjacent, they would occupy a substrate surface area given by $N_a/\psi = 0.83$ mm^2. Since the separation between the capacitors is 3.2 mm, such a localized avalanche would typically be recorded by only one capacitor, not both. In general, the spatial scale of an avalanche can be characterized by a radius R. For $R \approx 3.2$ mm (capacitor separation), we would expect to measure some correlated avalanche events on both capacitors. For $R \gg 3.2$ mm, the steps in capacitance recorded on the two capacitors would be expected to be strongly correlated in size. We observe strong correlations, with avalanches of similar size seen at the same time on each capacitor. A measure of this is the average of the ratio of the avalanche size for each member of the avalanche pairs, $\Delta C_1/\Delta C_2 = 1.08 \pm 0.33$. Thus, we conclude that these avalanche events are not localized events, but involve pores in dilute distribution across the entire sample. This conclusion is not anticipated by theories of percolated behavior in porous systems.

How do the interconnected but dispersed pores interact with one another and cause avalanche behavior? One possibility is interaction via the superfluid film on the Nuclepore surface which can support film thickness fluctuations large enough to stimulate pore draining. Another possibility is interaction via fourth sound (a superfluid density fluctuation) through the superfluid helium in the pores

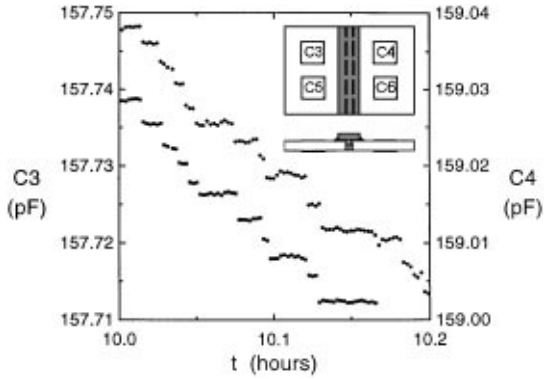

FIG. 3. Avalanche behavior for a pair of equal-sized capacitors, C3 (squares, bottom) and C4 (circles), located on separate Nuclepore samples (inset), connected by a nonporous bridge for $T_r = 1.424$ K shows correlated behavior. As noted in the text, the correlations disappear in the absence of the nonporous bridge.

themselves. Either of these possibilities might serve to disturb the stability of the fluid-vapor interface of those filled pores which are near to their stability limit [15] and thus cause them to drain. A third possibility might be draining via connectivity within the pore structure itself in which interconnected pores drain by means of the internal pore openings, leaving nearby pores filled. To examine the relevance of pore structure vs superfluid film connectivity, we created a third sample which consisted of four capacitors, two on each of two *separate* Nuclepore (200 nm pore diam) substrates (Fig. 3, inset). These separate substrates were joined to each other with a polycarbonate membrane (6 μm, no pores) which served as a bridge. The polycarbonate membrane was smoothly attached to the Nuclepore samples as a splice of width 2.54 mm with a 7.62 mm wide polycarbonate overlayer cemented in place with Apiezon N vacuum grease (which becomes glasslike at low temperatures). Thus, we were able to study (in the context of the labels on Fig. 3) regions of the sample connected by pores (e.g., C4 vs C6), and regions connected only by superfluid film (e.g., C3 vs C4). The results for C3 and C4, shown in Fig. 3, clearly show that the strong correlations seen in the experiment with two capacitors on a single Nuclepore sample (Fig. 2), and confirmed for this sample by measurements of C4 vs C6, persist when the capacitors are on *different* pieces of Nuclepore connected only by a nonporous bridge. In order to establish the irrelevance of possible external perturbations to the presence of correlated behavior, we removed the nonporous bridge and made measurements with the entirely separate and disconnected C3 and C4. Avalanches of similar size to the previous measurements were again observed on C3 and C4, but they were completely uncorrelated. Thus, these double-capacitor experiments unambiguously show that the correlations in avalanche behavior among the pores are enabled by the presence of the mobile superfluid film which connects the pores, and not by the presence of the porous structure itself nor by external disturbances to the system. For such a film connection, the draining of pores apparently launches a film fluctuation which stimulates other pores which are then included in the avalanche. This stimulation can extend beyond the edge of the porous structure and induce avalanches on an attached neighboring substrate. A phenomenological theory which models this process and successfully displays some of the features seen in the avalanche data has recently been proposed [21].

The draining of superfluid ^{4}He from Nuclepore is the first observed example of avalanches occurring in the draining of an adsorbing fluid from a porous material. Adsorption/draining experiments with ordinary fluids have not shown such behavior. For our geometry, avalanche events involve up to $\sim 2 \times 10^7$ pores. In an effort to characterize the avalanches, we have reported the avalanche size as a function of the amount of ^{4}He in the pores and the size distribution functions, and find that the size distribution function can exhibit power law behavior over a modest range in avalanche size. Measurements with two capacitors on the same sample indicate that the avalanches occur as dilute collections of pores which span the entire sample, a result which is inconsistent with simple invasion percolation models of avalanche events. A test of whether such correlated avalanches are due to the porous structure itself or instead are caused by a long range coupling mechanism due to the superfluid shows that it is the superfluid film rather than the porous structure *per se* which provides the coupling. By modifying the properties of this superfluid connection, by changing the ^{3}He-^{4}He concentration, or the temperature, for example, it should be possible to control the strength of the interaction, an advantage not present in most other systems.

We acknowledge useful discussions with R. A. Guyer and J. Machta. This work was supported by NSF via DMR 94-22208.

[1] E. Vives *et al.*, Phys. Rev. Lett. **72**, 1694 (1994).
[2] A. H. Thompson, A. J. Katz, and R. A. Raschke, Phys. Rev. Lett. **58**, 29 (1987).
[3] P. J. Cote and L. V. Meisel, Phys. Rev. Lett. **67**, 1334 (1991); L. V. Meisel and P. J. Cote, Phys. Rev. B **46**, 10 822 (1992); J. S. Urbach, R. C. Madison, and J. T. Markert, Phys. Rev. Lett. **75**, 276 (1995).
[4] S. Field, J. Witt, F. Nori, and X. Ling, Phys. Rev. Lett. **74**, 1206 (1995); W. Wu and P. W. Adams, Phys. Rev. Lett. **74**, 610 (1995).
[5] J. P. Sethna *et al.*, Phys. Rev. Lett. **70**, 3347 (1993); O. Perković, K. Dahmen, and J. P. Sethna, Phys. Rev. Lett. **75**, 4528 (1995).
[6] G. Mason, Proc. R. Soc. London A **415**, 453 (1988).
[7] R. A. Guyer and K. R. McCall, Phys. Rev. B **54**, 18 (1996).
[8] W. D. Machin, Langmuir **10**, 1235 (1994).
[9] J. H. Page *et al.*, Phys. Rev. Lett. **71**, 1216 (1993).
[10] Costar Corporation, Cambridge, MA.
[11] M. P. Lilly, P. T. Finley, and R. B. Hallock, Phys. Rev. Lett. **71**, 4186 (1993).
[12] J. M. Valles, Jr., D. T. Smith, and R. B. Hallock, Phys. Rev. Lett. **54**, 1528 (1985).
[13] D. T. Smith, K. M. Godshalk, and R. B. Hallock, Phys. Rev. B **36**, 202 (1987).
[14] K. M. Godshalk and R. B. Hallock, Phys. Rev. B **36**, 8294 (1987).
[15] W. F. Saam and M. W. Cole, Phys. Rev. B **11**, 1086 (1975); S. M. Cohen, R. A. Guyer, and J. Machta, Phys. Rev. B **33**, 4664 (1986).
[16] M. P. Lilly and R. B. Hallock, J. Low Temp. Phys. **101**, 385 (1995).
[17] M. P. Lilly and R. B. Hallock, Bull. Am. Phys. Soc. **41**, 436 (1996); M. P. Lilly and R. B. Hallock, in *Proceedings of the 21st International Conference on Low Temperature Physics* [Czech. J. Phys. **46**, Suppl. S1, 141 (1996)].
[18] S. J. Putterman, *Superfluid Hydrodynamics* (North-Holland, Amsterdam, 1974).
[19] M. P. Lilly and R. B. Hallock, Mater. Res. Soc. Symp. Proc. **366**, 241 (1995).
[20] D. S. Cannell and F. Rondelez, Macromolecules **13**, 1599 (1980).
[21] R. A. Guyer and K. R. McCall (to be published).